GeroScience (2022) 44:1891–1904
https://doi.org/10.1007/s11357-022-00585-5

ORIGINAL ARTICLE

Association of cerebral microvascular dysfunction and white matter injury in Alzheimer's disease

Zsolt Bagi · Christopher D. Kroenke · Katie Anne Fopiano · Yanna Tian · Jessica A. Filosa · Larry S. Sherman · Eric B. Larson · C. Dirk Keene · Kiera Degener O'Brien · Philip A. Adeniyi · Stephen A. Back

Received: 15 March 2022 / Accepted: 5 May 2022 / Published online: 25 May 2022

Abstract Patients with Alzheimer's disease (AD) often have cerebral white matter (WM) hyperintensities on MRI and microinfarcts of presumed microvascular origin pathologically. Here, we determined if vasodilator dysfunction of WM-penetrating arterioles is associated with pathologically defined WM injury and disturbances in quantitative MRI-defined WM integrity in patients with mixed microvascular and AD pathology. We analyzed tissues from 28 serially collected human brains from research donors diagnosed with varying degrees of AD neuropathologic change (ADNC) with or without cerebral microinfarcts (mVBI). WM-penetrating and pial surface arteriolar responses to the endothelium-dependent agonist bradykinin were quantified ex vivo with videomicroscopy. Vascular endothelial nitric oxide synthase (eNOS) and NAD(P)H-oxidase (Nox1, 2 and 4 isoforms) expression were measured with quantitative PCR. Glial fibrillary acidic protein (GFAP)-labeled astrocytes were quantified by unbiased stereological approaches in regions adjacent to the sites

Supplementary Information The online version contains supplementary material available at https://doi.org/10.1007/s11357-022-00585-5.

Z. Bagi (✉) · K. A. Fopiano · Y. Tian · J. A. Filosa
Department of Physiology, Medical College of Georgia, Augusta University, 1120 15th Street, Augusta, GA 30912, USA
e-mail: zbagi@augusta.edu

C. D. Kroenke
Advanced Imaging Research Center, Oregon Health & Science University, Portland, OR, USA

C. D. Kroenke · L. S. Sherman
Division of Neuroscience, Oregon National Primate Research Center, Oregon Health and Science University, Beaverton, OR, USA

L. S. Sherman
Department of Cell, Developmental and Cancer Biology, Oregon Health and Science University, Portland, OR, USA

E. B. Larson
Kaiser Permanente Health Research Institute, Seattle, WA, USA

E. B. Larson
Department of Medicine, University of Washington, Seattle, WA, USA

C. D. Keene
Department of Laboratory Medicine and Pathology, University of Washington School of Medicine, Seattle, WA, USA

K. Degener O'Brien · P. A. Adeniyi · S. A. Back (✉)
Department of Pediatrics, Oregon Health & Science University, Portland, OR, USA
e-mail: backs@ohsu.edu

S. A. Back
Department of Neurology, Oregon Health & Science University, Mail-Code L481, 3181 S.W. Sam Jackson Park Rd, Portland, OR 97239-3098, USA

of WM-penetrating vessel collection. Post-mortem diffusion tensor imaging (DTI) was used to measure mean apparent diffusion coefficient (ADC) and fractional anisotropy (FA), quantitative indices of WM integrity. In contrast to pial surface arterioles, white matter-penetrating arterioles from donors diagnosed with high ADNC and mVBI exhibited a significantly reduced dilation in response to bradykinin when compared to the other groups. Expression of eNOS was reduced, whereas Nox1 expression was increased in WM arterioles in AD and mVBI cases. WM astrocyte density was increased in AD and mVBI, which correlated with a reduced vasodilation in WM arterioles. Moreover, in cases with low ADNC, bradykinin-induced WM arteriole dilation correlated with lower ADC and higher FA values. Comorbid ADNC and mVBI appear to synergistically interact to selectively impair bradykinin-induced vasodilation in WM-penetrating arterioles, which may be related to reduced nitric oxide- and excess reactive oxygen species-mediated vascular endothelial dysfunction. WM arteriole vasodilator dysfunction is associated with WM injury, as supported by reactive astrogliosis and MRI-defined disrupted WM microstructural integrity.

Keywords Aging · Alzheimer's disease · White matter · Microvascular · Dilation · Astrocyte · MRI

Introduction

Clinical and experimental studies support that vascular dysfunction not only worsens, but plays a mechanistic role in the development of cognitive decline and dementia in patients with Alzheimer's disease (AD) [1–4]. Vascular contributions to cognitive impairment and dementia (VCID) are highly prevalent in individuals 75 years of age or older [1, 5]. VCID is accompanied by impairment in cognitive and executive function of presumed cerebral microvascular origin, which comprises a spectrum of subcortical small vessel disease that contributes to progressive injury of the periventricular and frontal white matter (WM) [6–10]. In addition to the abnormalities in the cerebral cortex, such as neuron loss and decreased synaptic density, clinical observations also suggest that alterations in the cerebral WM contribute to the development of cognitive dysfunction and memory deficits in AD [5, 11, 12]. Notably, a large proportion of AD patients exhibit co-morbid cardiovascular risk factors (i.e., hypertension, diabetes mellitus, and dyslipidemias) that are known to impair cerebral microvascular function. Cerebral small vessel disease is a common manifestation of aging and other cardiovascular disorders that cause cerebral hemodynamic disturbances, leading to reduced cerebral WM perfusion and subsequent axonal damage [1–4]. Myelination deficits can manifest as WM lesions or WM hyperintensities, detected by neuroimaging [8, 13–21]. Apparent differences in WM hyperintensities in elderly patients with AD coincide with diffusion tensor imaging (DTI)-measured fractional anisotropy (FA) abnormalities as an independent determinant of axonal loss [22]. Furthermore, individuals with AD pathology may not develop dementia without underlying vascular dysfunction. Human autopsy findings suggest that over 50% of clinical AD patients have histopathology- or MRI-defined vascular brain injury [23, 24]. Presently unresolved is the extent to which cerebrovascular dysfunction is associated with changes in WM integrity that affect cognitive and memory functioning in AD patients.

Consistent with the contribution of cerebral microvascular dysfunction to human WM injury, we previously described selective vasodilator dysfunction of WM penetrating arterioles, which appears to contribute to remyelination failure in chronic WM lesions in brain donors with no pathologically described macroscopic infarcts or hemorrhages and with low levels of AD neuropathologic change (ADNC) [24]. Earlier, we also identified significant oxidative damage to myelin and axons in WM, which, independent of the burden of ADNC, coincided with DTI-defined WM lesions [25]. While strong associations between oxidative stress and WM injury in chronic hypertension and diabetes support a microvascular etiology in both VCID and AD [1, 26], the role of microvascular dysfunction in the development of WM injury from co-morbid pathologies of VCID and AD remains undefined. Here, we hypothesized that vasodilator dysfunction of WM-penetrating arterioles is closely linked with quantitative MRI/DTI-defined WM integrity and astrogliosis, especially in patients exhibiting both microvascular brain injury (mVBI) and high ADNC. To test this hypothesis, we analyzed prefrontal WM of deceased older participants in a population-based cohort focused on understanding the epidemiology and biological underpinnings of brain

aging and dementia. In contrast to pial arterioles, we found that a selectively impaired, bradykinin-induced vasodilation occurs in WM-penetrating arterioles from brain donors with comorbid ADNC and microvascular brain injury. Abnormal vasodilator responses of WM penetrating arterioles were associated with pathological confirmation of WM injury and MRI-defined WM microstructural integrity changes.

Materials and methods

Subjects and tissue handling

All tissues were derived from brains donated for research by participants in the Kaiser Permanente Washington Health Research Institute Adult Changes in Thought (ACT) study, an ongoing population-based study of aging and incident dementia among men and women in Seattle, WA. For vascular reactivity studies, between 2013 and 2016, we prospectively collected 28 human WM samples at the level of prefrontal cortex (PFC) from rapid research brain collections and protocols customized for this study in the University of Washington Bio Repository and Integrated Neuropathology Laboratory. Superior frontal gyrus and subcortical white matter from one randomly determined hemisphere from donors with short post-mortem interval were rapidly dissected, immersed in ice-cold artificial cerebrospinal fluid (aCSF), and shipped to Augusta University for vascular reactivity studies and analyses, as previously described [24]. Adjacent prefrontal subcortical and deep white matter were dissected rapidly, flash frozen in liquid N_2 or fixed in 4% paraformaldehyde (followed 48 h later by transfer to PBS), and shipped to Oregon Health Sciences University for molecular and stereological analyses. Post-mortem intervals were < 8.3 h to tissue collection and preservation. After the rapid procedures, the intact hemibrain, and remaining non-sampled dissected hemisphere, were fixed in 10% neutral buffered formalin (NBF), followed by systematic tissue sectioning, sampling, and extensive histological and immunohistochemical workup according to the NIA-AA (National Institute on Aging-Alzheimer's Association) guidelines for the assessment of ADNC [27, 28], which includes assessment of microvascular brain injury (mVBI), as defined by the number of cerebral microinfarcts in standard screening Sections [29–31]. We excluded other commonly comorbid pathological changes in the aging brain, including Lewy body disease and gross infarcts or chronic hemorrhages. Inclusion criteria for vascular reactivity studies took into consideration the impact of vascular and parenchymal amyloid and employed the NIA-AA criteria and scoring for cerebral amyloid angiopathy (CAA) by evaluation of amyloid (A)β immunohistochemistry in leptomeningeal and parenchymal vessels. In addition to overall ADNC, we focused specifically on Braak stage of neurofibrillary degeneration as used in our past studies. For both cohorts, cases with cortical, WM, basal ganglia, or thalamic microinfarcts were assigned to the mVBI group (Table 1).

Videomicroscopic assessment of cerebral arterioles

Pial surface and WM-penetrating arterioles were dissected from PFC samples and maintained at 37 °C in Krebs solution (mmol/L): 110 NaCl, 5.0 KCl, 1.25 $CaCl_2$, 1.0 $MgSO_4$, 1.0 KH_2PO_4, 5.0 glucose, and 24.0 $NaHCO_3$ equilibrated with 21% O_2/5% CO_2, pH 7.4. Microvessels were cannulated on both ends and mounted on glass micropipettes connected to a pressure servo controller. Internal arteriolar diameter at the midpoint of the arteriolar segment was measured by videomicroscopy with a microangiometer (Living Systems Instrumentation) [32, 33]. After 1 h equilibration, internal arteriolar diameter (ID) was measured in response to step increases in intraluminal pressure from 20 to 120 mmHg (20 mmHg pressure increments) in the presence of normal Ca^{2+} (1.25 mM) and absence of extracellular Ca^{2+} concentrations (Ca^{2+} free Krebs solution, passive arteriolar diameter). Arterioles (50 mmHg intraluminal pressure) were pre-constricted with thromboxane A_2 analog, U46619 (3×10^{-8} mol/L) to induce ~ 30% of arteriolar tone. Cumulative concentrations of the endothelium-dependent agonist, bradykinin (BK, 10^{-9}–10^{-6} mol/L) was administered and arteriolar diameter changes measured. Maximally developed percent changes in vasodilatation were calculated $[(ID_{maximal} - ID_{initial})/(ID_{passive} - ID_{initial}) \times 100)]$.

RT-qPCR

Total RNA was extracted from fast-frozen pial surface and WM-penetrating arteries using Trizol (Invitrogen Life Technologies, Carlsbad, CA)

Table 1 Donor characteristics, neuropathology, and vascular dimensions. Data presented as number (*n*) percent (%), or mean ± standard deviation. No mVBI is defined as no infarcts (territorial, lacunar, CMIs). mVBI is defined as any CMIs as depicted in Fig. 1. AD is defined as NIA-AA ADNC intermediate or high. Abbreviations: *mVBI* microvascular vascular brain injury, *AD* Alzheimer's disease, *No.* number of subjects, *Age* average age at death, *Ventricular Diameter* left ventricular diameter at temporal tips, *CAA* cerebral amyloid angiopathy, *NIA-AA* National Institute on Aging and Alzheimer's Association. Fisher's exact test is used for the categorical variables, and 2-sample *t*-test is used for the continuous variables. $P < 0.05$ *, compared to control; †, compared to mVBI

	Control	mVBI	AD	AD + mVBI
Number (n) of donors	6	7	8	7
Age (years)	89.0 ± 5.7	89.7 ± 4.3	89.7 ± 7.3	87.9 ± 15.7
Female:male	4:2	3:4	6:2	6:1
Post-mortem interval (hours)	4.83 ± 1.32	4.55 ± 0.6	5.33 ± 1.7	4.86 ± 1.7
Brain weight (grams)	1189 ± 105	1183 ± 86	1146 ± 131	1102 ± 97
CAA				
None, *n*, (%)	5 (83)	4 (57)	4 (50)	3 (43)
Mild, *n*, (%)	1 (17)	3 (43)	1 (13)	1 (14)
Moderate, *n*, (%)	0 (0)	0 (0)	3 (38)	2 (29)
Severe, *n*, (%)	0 (0)	0 (0)	0 (0)	1 (14)
Thal Aβ phase				
0, *n*, (%)	3 (50)	2 (29)	0 (0)	0 (0)
1 or 2, *n*, (%)	2 (33)	1 (14)	0 (0)	0 (0)
3, *n*, (%)	0 (0)	2 (29)	2 (25)	1 (14)
4 or 5, *n*, (%)	1 (17)	1 (14)	6 (75)†	6 (86)*†
CERAD				
Absent, *n*, (%)	3 (50)	4 (57)	0 (0)†	0 (0)
Sparse, *n*, (%)	1 (17)	1 (14)	3 (38)	0 (0)
Moderate, *n*, (%)	1 (17)	0 (0)	2 (25)	1 (14)
Frequent, *n*, (%)	1 (17)	1 (14)	3 (38)	6 (86)*†
Braak NFT stage				
I/II, *n*, (%)	4 (67)	3 (43)	0 (0)*	0 (0)*
III/IV, *n*, (%)	2 (33)	4 (57)	3 (38)	1 (14)
V/VI, *n*, (%)	0 (0)	0 (0)	5 (63)*†	6 (86)*†
NIA-AA ADNC				
Not or low, *n*, (%)	6 (100)	7 (100)	0 (0)*†	0 (0)*†
Intermediate, *n*, (%)	0 (0)	0 (0)	4 (50)	2 (29)
High, *n*, (%)	0 (0)	0 (0)	4 (50)	5 (71)*†
Pial artery diameters (in μm)				
Active (Ca^{2+} plus)	83 ± 25	94 ± 54	86 ± 40	88 ± 26
Passive (Ca^{2+} free)	137 ± 47	141 ± 56	138 ± 88	106 ± 45
WM artery diameters (in μm)				
Active (Ca^{2+} plus)	70 ± 13	71 ± 9	60 ± 21	66 ± 40
Passive (Ca^{2+} plus)	106 ± 24	120 ± 36	100 ± 41	101 ± 42

and assessed for RNA purity using NANO Drop. Complementary DNA was synthesized from 1 μg purified RNA using oligo(dT) primers and the SuperScript III First-Strand Synthesis System for RT-PCR (Invitrogen Life Technologies, Carlsbad, CA). Primers used for analysis for eNOS and NOX1-4 were chosen from primer pairs designed with BLAST. Quantitative real-time PCR was performed with SYBR green (Bio-Rad Laboratories, Hercules, CA) on a Bio-Rad CFX Connect Real-time PCR detector. Amplification was performed in duplicate at 95 °C for 3 min, followed by 45 cycles at 95 °C for 15 s, 58.5 °C for 15 s, and 72 °C for 15 s. The relative gene expression of individual target genes was calculated using the $2^{-\Delta\Delta ct}$ method against a human 18S ribosomal RNA.

Immunohistochemistry and stereological quantification of N_v

After MRI studies were completed, tissue blocks were serially sectioned free-floating (50 μm) in PBS

with a Leica VTS-1000 vibrating microtome. After antigen-retrieval [34], three tissue sections per case were incubated for 48 h at 2–4 °C in mouse anti-human GFAP (1:500; Merck-Millipore). Tissue sections were incubated in goat anti-mouse secondary antibody (1:200; Vector) and processed for immunoperoxidase staining [34]. Estimation of numerical cell densities (N_v) for GFAP-labeled somata was accomplished with the optical fractionator using detailed protocols for (1) delineation and systematic random sampling of regions-of-interest; (2) section thickness measurements; (3) counting brick construction; and (4) counting procedures [34].

Ex vivo diffusion tensor magnetic resonance imaging

Tissue was immersed in PBS within a 2.5-cm diameter tube. A 3.5-cm diameter, 3.5-cm in length, single-turn solenoidal coil was utilized for radiofrequency transmission and reception. Experiments were performed using a 11.7 T magnet interfaced with a 9-cm inner diameter magnetic field gradient coil (Bruker, Rheinstetten, Germany). A Stejskal-Tanner multi-slice spin-echo pulse sequence was used to perform DTI measurements utilizing 3 b-values of 2.5, 5.0, and 7.5 ms/μm^2. For each b-value, a 25-direction, icosahedral sampling scheme, in combination with two measurements in which b = 0, was utilized. Other pulse sequence settings were TR = 9 s, TE = 42 ms, NEX (the number of averaged transients) = 1, and image resolution was isotropic, with voxel dimensions of (0.5 mm)^3 and a 32 (phase-encode) by 64 (readout) by 30 mm (slice-select) field of view. A Hanning filter was applied to the k-space data prior to Fourier transformation in the readout and phase-encode directions to minimize Gibbs ringing intensity variations arising from sharp transitions in intensity between tissue and PBS. Data were then analyzed with standard DTI formulas [35] to obtain ADC and FA parameter maps. Voxels within WM for each tissue block were manually classified by an individual who was blinded to neuropathologic classification using the image comprised of the average of the 6 b = 0 images with ITK-snap [36] (http://www.itksnap.org/pmwiki/pmwiki.php). Mean values for DTI-derived parameters within WM reported herein for a given case are computed as means over the set of voxels classified as WM.

Statistical analysis

Vascular studies Data are expressed as mean ± SEM. Statistical analysis employed GraphPad Prism Software by one-way ANOVA followed by Tukey post hoc test, or Student's *t*-test. If normal data distribution was met (Kolmogorov–Smirnov), Pearson's correlation and linear regression analyses were performed. For data not meeting normal distribution, Spearman's correlations were used.

GFAP studies Statistical analysis employed SAS software 9.2. To compare group means, unpaired two-tailed Student's *t*-tests were performed.

Results

Features of cases from a population-based autopsy cohort

From 28 prospective cases that were consecutively collected in a blinded study design, we identified cases with NIA-AA intermediate or high ADNC

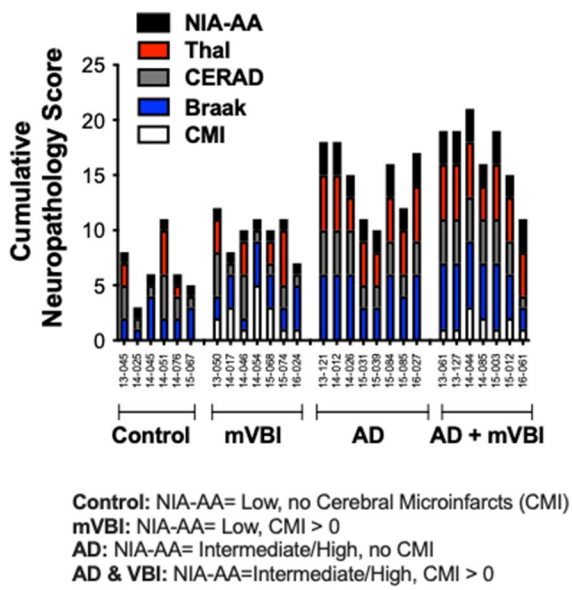

Fig. 1 Burden of AD and mVBI for each of 28 cases ranked by a cumulative neuropathology score based on NIA-AA score (1–3; low to high), Thal phase (0 to 5), CERAD score (1–3; sparse to frequent), Braak stage for neurofibrillary tangles (I–VI), and the sum of CMIs

(AD, $n=8$), no or low ADNC and mVBI (mVBI, $n=7$), intermediate or high ADNC and mVBI (AD plus mVBI, $n=7$), and control (no or low ADNC and no mVBI, $n=6$) based on a detailed neuropathologic evaluation (Table 1). Figure 1 depicts the cumulative neuropathological scores in the four groups.

Selectively impaired bradykinin-induced WM arteriole dilation in AD plus mVBI cases

Baseline diameters of pial and WM-penetrating arterioles were similar in cases of AD with or without mVBI when compared to controls, both in the presence of Ca^{2+} (active diameters at 50 mmHg) and absence of Ca^{2+} (passive diameters at 50 mmHg) (Table 1). Vasodilation in response to bradykinin was similar in pial arterioles regardless of AD or mVBI, when compared to controls (Fig. 2A). However, dilation of WM penetrating arterioles to increasing concentrations of bradykinin, an endothelium-dependent agonist, was significantly reduced in the AD plus mVBI group (Fig. 2B). Pial and WM-penetrating arteriole responses to bradykinin were not significantly influenced by patient age or post-mortem interval (Supplemental Figure I).

WM arteriole dilator dysfunction is accompanied by changes in eNOS and Nox1 expression

To determine the potential underlying mechanisms of the selectively impaired dilator function in WM-penetrating arterioles, gene expression of vascular endothelial nitric oxide synthase (eNOS) and NAD(P)H-oxidase (Nox1, 2 and 4 isoforms) was measured with quantitative PCR. We found a trend for a reduced expression of eNOS in pial and WM-penetrating arterioles in cases with AD and mVBI when compared to controls (Fig. 3A). Nox1 expression showed a trend towards increased expression only in WM arterioles in AD and mVBI cases (Fig. 3B). There were no changes detected in the expression of Nox2 and Nox4 among the cases (Fig. 3C & D). These data suggest that altered eNOS and Nox1 levels contribute to alterations in the WM arteriole dilation in AD and mVBI.

WM arteriole dysfunction is accompanied by astrogliosis in cases with AD and mVBI

We previously reported that mVBI WM lesions displayed an increase in GFAP-labeled astrocytes in the prefrontal WM [24]. We therefore determined the extent of astrogliosis in cases with AD and mVBI, which also displayed WM-penetrating arteriole dysfunction. We quantified GFAP-labeled astrocytes in the prefrontal WM (Fig. 4A–D) and found a significant increase in astrocyte density for AD and mVBI vs. controls (Fig. 4E). The mixed presence of AD and mVBI coincided with the highest magnitude of WM injury as defined by astrocyte density (Fig. 4E). Analysis of the entire cohort

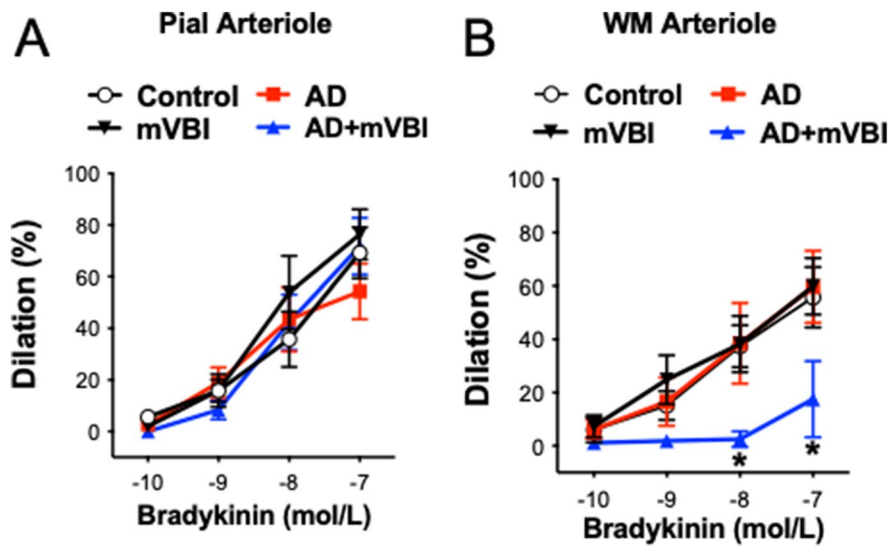

Fig. 2 Summary data of vasodilation in response to cumulative concentrations of bradykinin (10^{-10} to 10^{-7} mol/L) is shown in pial surface (**A**) versus WM-penetrating arterioles (**B**) in the control ($n=6$), mVBI ($n=7$), AD ($n=8$), and mVBI plus AD ($n=7$) groups. *$P<0.05$ compared to control, mVBI, or AD

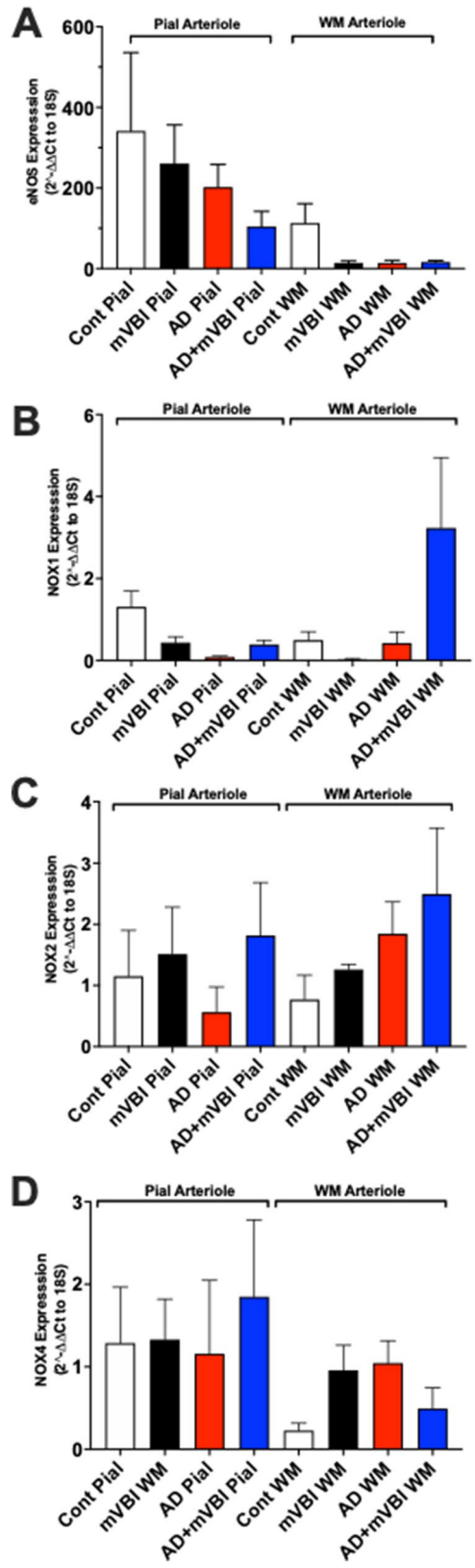

Fig. 3 Expression of vascular endothelial nitric oxide synthase (**A**; eNOS) and NAD(P)H-oxidase (Nox1, 2 and 4 isoforms; **B**–**D**) measured by qPCR in pial and WM-penetrating arterioles for control, mVBI, AD, and mVBI + AD cases ($n = 4$ per group)

showed a trend towards a negative correlation ($P = 0.057$, $r - 0.44$, Pearson correlation) between the magnitude of WM arteriole dilation and white matter astrocyte density (Fig. 4F).

WM arteriole dysfunction correlates with quantitative MRI-defined changes in WM integrity

We next determined if dysfunction of WM-penetrating arterioles correlates with WM microstructural integrity changes in cases with AD and mVBI. We used ex vivo DTI on fixed brain tissue samples to measure the ADC and FA in prefrontal WM. In the whole cohort, there was only a trend towards the anticipated negative correlation ($P = 0.067$, $r - 0.43$, Pearson correlation) between the magnitude of bradykinin-induced WM arteriole dilation and ADC (Fig. 5A). No associations were observed between WM arteriole dilations and FA (Fig. 5B), whereas a positive correlation would be expected if bradykinin response corresponded to WM integrity. We found however that the anticipated negative correlation with ADC and positive correlation with FA were observed in cases with low ADNC (Fig. 5C, D). In contrast, in cases with high ADNC where the dynamic range of vasodilator responses to bradykinin was much lower and limited, associations with DTI parameters were not found.

Discussion

This study was conducted in prospectively and consecutively collected samples from a community-based cohort followed until death with brain aging and incident dementia. We report that a selectively impaired vasodilation to the endothelium-dependent agonist bradykinin occurs in WM-penetrating arterioles in cases with high ADNC and comorbid mVBI (cases with cerebral microinfarcts). The impaired vasodilator response of WM arterioles in AD and mVBI is associated with WM injury, as confirmed by astrogliosis and DTI-measured changes in WM

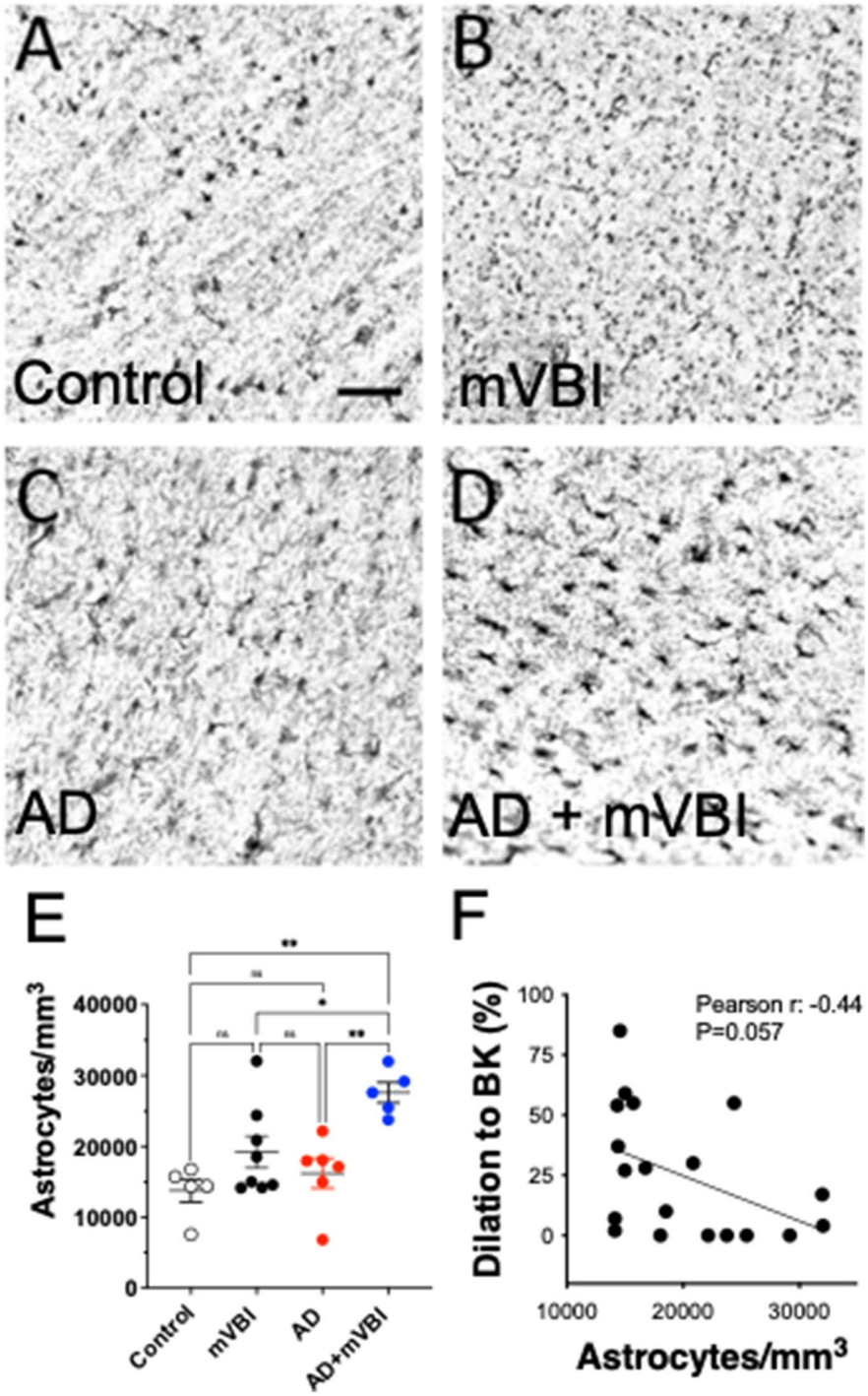

Fig. 4 WM arteriole dysfunction is accompanied by significant elevations in astrocyte density in AD + mVBI (**D**) vs. control (**A**), mVBI (**B**), and AD only (**C**) groups as illustrated with representative photomicrographs of GFAP-labeled astrocytes (**A**–**D**) and shown quantitatively in E (*$P < 0.05$; **$P < 0.01$; NS = nonsignificant). **F** Bradykinin-mediated vasodilation of WM arterioles plotted vs. astrocyte density, as a marker of the burden of WMI. Scale bar, 100 μm

microstructural integrity. These findings suggest a synergistic, detrimental effect of ADNC and mVBI on WM arteriole vasodilator function and associated WM injury, which could contribute to enhanced risk for cognitive dysfunction and dementia.

We previously reported that mVBI is accompanied by oxidative stress and quantitative MRI-defined abnormalities in prefrontal WM that involve disrupted integrity of axons and myelin [25]. In a subsequent study, we found that human mVBI involves an

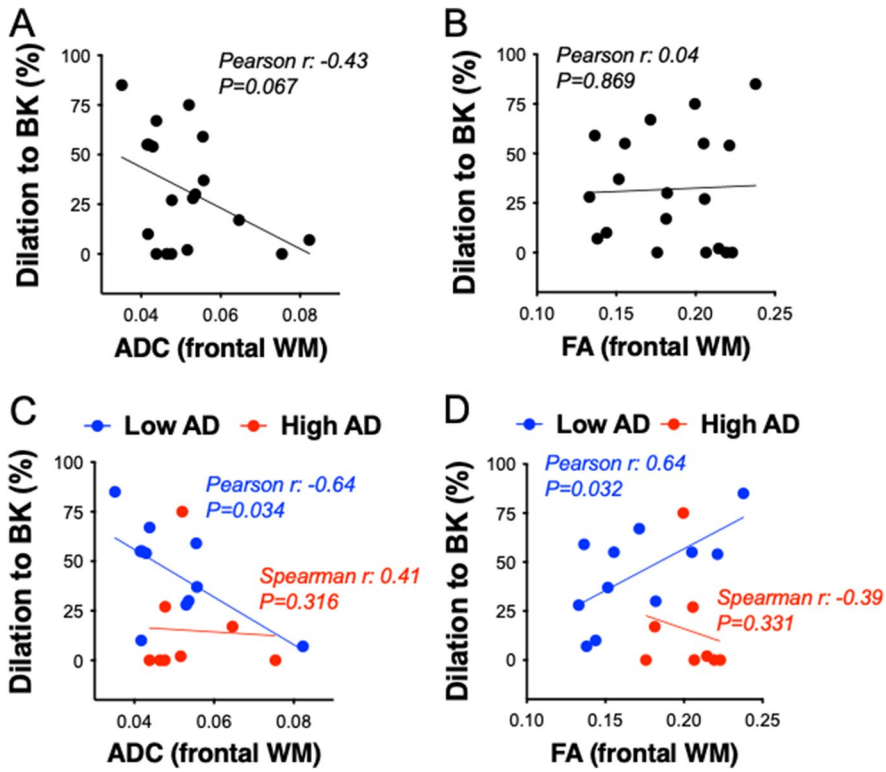

Fig. 5 Bradykinin-induced vasodilation of WM arterioles for the entire cohort of cases plotted vs. MRI-defined frontal white matter apparent diffusion coefficient (ADC; **A**) and fractional anisotropy (FA; **B**). **C**, **D** Bradykinin-mediated vasodilation of WM arterioles is plotted for the low AD vs. high AD cases, which illustrates the loss of vasomotor response in the high AD group in contrast to low AD, which is significantly associated with bradykinin response for both ADC (**C**) and FA (**D**)

unexpected imbalance in vascular reactivity between pial and WM microvessels, and that impaired vasodilator function of WM-penetrating arterioles was associated with WM lesions in which oligodendrocyte progenitors failed to terminally differentiate to myelinating oligodendrocyte in astrocyte-enriched lesions [24].

Recent evidence suggests that individuals with high ADNC (Aβ deposition and pathologic tau) may not develop dementia without underlying cerebrovascular dysfunction [37], which may not only worsen but also play a mechanistic role in the development of cognitive decline and dementia in patients with AD. While strong associations between cerebral small vessel disease and WM injury suggest such a mechanistic link, the contributions of cerebral vascular dysfunction and human AD remain poorly defined. It has been long recognized that many AD patients exhibit co-morbid cardiovascular disease, including hypertension and diabetes mellitus that are well-known contributors to cerebral microvascular endothelial dysfunction [1–4]. In these pathological conditions, disrupted cerebral perfusion may arise even before the development of substantial neuronal and axonal damage and cognitive dysfunction. On the other hand, studies also have shown a significantly reduced cerebral blood volume in young (4-month-old) transgenic mutant amyloid precursor protein (APP) mice, indicating that very early disturbances in the microvasculature occur in the hippocampus and cerebral cortex in this AD mouse model [38]. Interestingly, aged mice overexpressing mutant or even non-mutant forms of tau also develop both morphological and functional pathological changes in cerebral cortex blood vessels [39]. Collectively, emerging experimental evidence suggests that early changes in cerebral microvascular function occur and may be mechanistically linked to ADNC.

In this study, we determined the function of WM-penetrating arterioles in donors exhibiting both microvascular brain injury (mVBI) and low or high ADNC and defined the relationship between vascular dysfunction, astrogliosis, and quantitative MRI-measured WM microstructural integrity. Most human cerebrovascular functional reactivity studies examined only larger caliber vessels such as the middle cerebral [40, 41] and pial arteries [42]. In the present study, pial arterioles had no apparent defects in vascular reactivity, but WM arterioles displayed an impaired

dilation to the endothelium-dependent agonist, bradykinin in cases with mVBI, and high ADNC. Since pial arterioles regulate downstream changes in local WM flow [1], our results suggest that additional compromise of arteriolar blood flow involves dysregulation of blood flow at the level of penetrating WM arterioles, especially with WM injury from both mVBI and high ADNC. Moreover, impaired endothelial function of WM arterioles may also limit the retrograde, upstream propagation of vasodilator signaling, thereby preventing both local and pial surface artery-dependent control of cerebral blood flow in ADNC, as previously suggested [43, 44]. Cerebrovascular endothelial cells are integral part of the neurovascular unit. Through a dynamic communication with cerebrovascular smooth muscle cells, astrocytes, and neurons, endothelial cells critically contribute to the moment-to-moment regulation of cerebral blood flow [45]. In addition, hemodynamic forces acting through vascular endothelial cells, such as wall shear stress, can also modify glial and neuronal functioning to maintain cerebral homeostasis [45]. It has been long known that ischemic WM lesions often occur in watershed areas supplied by WM penetrating arteries [46]. Under pathological conditions, subcortical WM is considered even more vulnerable to reduced perfusion and less capable of tolerating fluctuations of cerebral blood flow and cerebral venous pressure [47]. It is therefore plausible that cerebrovascular endothelial cell dysfunction occurring selectively in WM-penetrating arterioles not only exaggerates but also contributes to the development of WM injury in AD patients.

The mechanisms of impaired vasodilation of WM penetrating arterioles that contribute WM injury remain poorly defined but appear to be exacerbated by the combination of ADNC and mVBI. Notably, transgenic mice overexpressing APP display pronounced disturbances in cerebral autoregulation [48]. Endothelial synthesis of the vasodilator NO by the endothelial NO synthase (eNOS) is central to dilation of cerebral arteries [49] and plays key roles in cerebrovascular regulation related to cognitive impairment [50]. We previously found a significant elevation in WM oxidative stress in mVBI, independent of the burden of AD, but associated with WM lesions [25]. APP transgenic mice with elevated soluble Aβ levels display markedly reduced cerebrovascular responses to vasodilatory stimuli [48, 51–55]. In endothelium-specific APP-deficient (eAPP−/−) mice, NO-mediated endothelium-dependent vasodilation was reduced, which was accompanied by reduced eNOS expression and cGMP levels [56]. Notable, endothelial dysfunction was found to be preserved in transgenic mice expressing both mutant pathogenic APP and superoxide dismutase-1 (SOD1), supporting a role for excess production of reactive oxygen species in mutant APP transgene mice. In this context, it has been shown that in cerebral microvessels of transgenic mice expressing the Swedish double mutation of human APP (Tg2576 mice) leads to eNOS uncoupling, which is a potential source of superoxide anion production [57]. NAD(P)H oxidases (Nox1–4) are another source of reactive oxygen species that can directly interfere with NO-mediated vasodilation, and thus contribute to the development of cerebrovascular dysfunction in transgenic mice that overexpress abnormal APP [58, 59]. Here, we report a trend for a reduced expression of eNOS in WM-penetrating arterioles, when compared to pial vessels and also in WM arterioles in human cases with ADNC and mVBI. Moreover, Nox1 expression showed a trend towards increased expression only in WM arterioles in ADNC and mVBI, when compared to other groups of cases. These findings suggest a role for augmented oxidative stress-related impairment of WM-penetrating arteriole function, which may be attributed to a synergistic interaction between mVBI and ADNC, but to demonstrate causation additional mechanistic studies with a larger cohort are required to further explore this possibility.

We also examined whether changes in WM microvascular vasomotor function correlate with neuroimaging parameters of cerebral WM microstructural integrity. Although MRI-defined WM hyperintensities are commonly detected in periventricular as well as frontal WM, the pathological features for these lesions remain poorly defined [60, 61]. Studies have begun to determine the spectrum of MRI-defined hyperintensities and other quantitative MRI indices of WM injury in AD patients. A prior study by Gouw et al. found considerable heterogeneity in WM hyperintensities in elderly patients with AD and observed that DTI-measured FA was the only independent determinant of axonal loss [22]. We previously analyzed frontal WM lesions by diffusion-based ex vivo high-field quantitative MRI and found that cases with mVBI and low AD

pathology displayed no abnormalities, but a significant loss of FA was detected in cases with mVBI and high AD pathology [25]. In the present study, we examined the associations between vasodilator function of WM-penetrating arterioles and quantitative DTI parameters (ADC and FA) in cases with mVBI and ADNC mixed pathology. In cases with low ADNC (with or without mVBI), the magnitude of WM arteriole dilation was significantly correlated with higher FA and lower ADC values, indicating that vasomotor dysfunction was closely associated with pathological microstructural changes in the WM in these cases. Interestingly, the association between penetrating arteriole dilation and FA and also ADC were lost in cases with high ADNC, which can be due to the markedly reduced vasodilator responses of WM arterioles in most of these cases. These observations suggests that ADNC-related pathological changes in the WM may better correlate with microvascular vasodilator dysfunction when compared to MRI-detected WM microstructural changes in patients with high ADNC.

Limitations

One limitation of our study was the small sample size for studies of gene expression of pial surface and WM penetrating arterioles, which yielded acceptable RNA quality only in four subjects in each group. These studies were not sufficiently powered to provide plausible links for the impaired vasomotor reactivity observed in this study. It should be also noted that assessment of eNOS and NOX gene expression does not directly indicate the bioavailability of NO, which should be evaluated in future mechanistic studies. We also note that in the present study, bradykinin was used as a pharmacological agonist to assess the magnitude of endothelium-dependent vasodilation in isolated cerebral arteries. Interestingly, under pathological conditions, bradykinin plays multiple roles in the neurovascular unit, including regulation of blood brain barrier permeability and inflammatory cytokine release that may also contribute to astrocyte and microglial activation [62]. The role of bradykinin in mixed vascular (mVBI) and ADNC in affecting WM-penetrating arteriole vasomotor response and other AD-related pathological changes in the neurovascular unit has yet to be elucidated. In addition, the small sample size for the four patient groups also limited the analysis of associations related to microvascular vasodilator dysfunction and MRI-detected abnormal WM microstructural changes.

Perspectives

Our study supports a role for independent and synergistic contributions of mVBI and AD to cerebral microvascular and AD neuropathological changes in aging human brain. Since there are no reliable tissue biomarkers for mVBI, our results suggest the utility of cerebral microvascular endothelial dysfunction to determine the extent of mVBI in autopsy cases, which can be used to stratify patients and also define correlations with neuropathological and noninvasive neuroimaging parameters. While the mixed effects of AD and mVBI appear to have a synergistic impact on cerebral microvascular dysfunction and WM injury, several outstanding questions remain. Both AD and cardiovascular diseases, such as hypertension, diabetes mellitus, and heart failure, are similarly detrimental to the cerebral microvasculature, which undergoes pronounced functional and structural changes. The nature of the cellular and molecular mechanisms by which WM parenchymal arterioles are selectively affected and are more vulnerable and less capable of tolerating fluctuations of cerebral blood flow under the combination of these pathological conditions is an area of active investigation. Underlying mechanisms through which WM-penetrating arteriole dysfunction leads to WM microstructural changes in patients with low or high ADNC also remain poorly understood. Consistent with this notion, in this study, we found that WM-penetrating arteriole responses to bradykinin were more significantly associated with MRI-defined diffusion changes in patients with low ADNC, but were lost in cases where vasomotor responses were mostly diminished in high ADNC. In this context, we previously found that vasodilator dysfunction of WM-penetrating arterioles is accompanied by reactive gliosis that involves astrocytes and microglia [24]. Dysfunction of WM-penetrating arterioles leads to hypoxia, inflammation, and oxidative/nitrosative stress that contribute to axon and myelin damage due to the failure in maturation of myelinating oligodendrocytes [24]. It is therefore possible that mixed mVBI and ADNC is accompanied by exaggerated damage selectively to the WM. Through

this process, it is also possible that vasomotor dysfunction of cerebral parenchymal arterioles as well as pathological hemodynamic changes, such as seen in hypertension, can lead to the direct, vascular cell-dependent activation of astrocytes [63, 64]. Cerebral WM microvascular-mediated phenotypic changes in astrocytes can also affect the upstream propagation of vasodilator signaling, thereby preventing both local (WM) and pial surface artery-dependent control of cerebral blood flow. This scenario however has yet to be demonstrated in human studies.

Taken together, our findings support that WM-penetrating arteriole dysfunction commonly occurs in aging-associated WM injury and raises the potential for worse cognitive dysfunction and memory deficits in patients with comorbid mVBI and AD. However, future functional imaging studies that simultaneously assess cerebral WM perfusion and test for cognitive function are needed to provide direct mechanistic links and insights. A better understanding of the molecular mechanisms of human cerebral microvascular dysfunction could lead to the identification of novel therapeutic targets, thereby offering novel avenues for targeted preventive strategies for VCID and AD.

Acknowledgements We thank Allison Beller and Aimee Schantz for superb administrative support, and Marta Balogh, Kim Howard, Lisa Keene, and Amanda Keen for outstanding technical support. We are very grateful to all the ACT participants and families without whose dedication to supporting critical human research this work would be impossible.

Author contribution Z.B., L.S.S., C.D.K., E.B.L., and S.A.B. conceptualized the project and were responsible for study design. Z.B., C.D.Kr., J.A.F., L.S.S., C.D.K., and S.A.B. wrote, edited, and finalized the manuscript. C.D.K. supervised all human pathology studies. Z.B., K.A.F., and Y.T. conducted vascular reactivity studies. K.D.O. and P.A. conducted astrocyte studies. C.D.Kr. conducted MRI/DTI studies.

Funding Supported by grants from the National Institute on Aging (AG054651 to ZB, AG065406 to SAB, AG031892, U01 AG006781 and U19 AG066567 which supports the ACT study, p50 AG005136 and p30AG066509, which support the UW Alzheimer's disease Research Center), the National Institute of Neurological Disorders and Stroke (NS105984 to SAB and NS054044 to C.D.K), and by the Nancy and Buster Alvord Endowment (to C.D.K). L.S.S was supported by NIH P51 OD011092. K.A.F was supported by NIH T32HL155011.

Data availability We declare that the data supporting the findings of this study are available within the article and its Supplementary Information files and from the corresponding authors upon request.

Declarations

Conflict of interest The authors declare no competing interests.

References

1. Iadecola C. The pathobiology of vascular dementia. Neuron. 2013;80:844–66.
2. Pimentel-Coelho PM, Rivest S. The early contribution of cerebrovascular factors to the pathogenesis of Alzheimer's disease. Eur J Neurosci. 2012;35:1917–37.
3. Jellinger KA. Prevalence and impact of cerebrovascular lesions in Alzheimer and lewy body diseases. Neurodegener Dis. 2010;7:112–5.
4. Snowdon DA, Greiner LH, Mortimer JA, Riley KP, Greiner PA, Markesbery WR. Brain infarction and the clinical expression of Alzheimer disease The Nun Study. Jama. 1997;277:813–7.
5. Corriveau RA, Bosetti F, Emr M, Gladman JT, Koenig JI, Moy CS, Pahigiannis K, Waddy SP, Koroshetz W. The science of vascular contributions to cognitive impairment and dementia (VCID): a framework for advancing research priorities in the cerebrovascular biology of cognitive decline. Cell Mol Neurobiol. 2016;36:281–8.
6. Rosenberg GA, Wallin A, Wardlaw JM, Markus HS, Montaner J, Wolfson L, Iadecola C, Zlokovic BV, Joutel A, Dichgans M, Duering M, Schmidt R, Korczyn AD, Grinberg LT, Chui HC, Hachinski V. Consensus statement for diagnosis of subcortical small vessel disease. J Cereb Blood Flow Metab. 2016;36:6–25.
7. De Silva TM, Faraci FM. Microvascular dysfunction and cognitive impairment. Cell Mol Neurobiol. 2016;36:241–58.
8. Conklin J, Silver FL, Mikulis DJ, Mandell DM. Are acute infarcts the cause of leukoaraiosis? Brain mapping for 16 consecutive weeks. Ann Neurol. 2014;76:899–904.
9. Lee S, Viqar F, Zimmerman ME, Narkhede A, Tosto G, Benzinger TL, Marcus DS, Fagan AM, Goate A, Fox NC, Cairns NJ, Holtzman DM, Buckles V, Ghetti B, McDade E, Martins RN, Saykin AJ, Masters CL, Ringman JM, Ryan NS, Frster S, Laske C, Schofield PR, Sperling RA, Salloway S, Correia S, Jack C, Weiner M, Bateman RJ, Morris JC, Mayeux R and Brickman AM. White matter hyperintensities are a core feature of Alzheimer's disease: evidence from the dominantly inherited Alzheimer network. Ann Neurol. 2016;79(6):929–39.
10. Smith EE, Salat DH, Jeng J, McCreary CR, Fischl B, Schmahmann JD, Dickerson BC, Viswanathan A, Albert MS, Blacker D, Greenberg SM. Correlations between MRI white matter lesion location and executive function and episodic memory. Neurology. 2011;76:1492–9.
11. Brundel M, de Bresser J, van Dillen JJ, Kappelle LJ, Biessels GJ. Cerebral microinfarcts: a systematic review of neuropathological studies. J Cereb Blood Flow Metab. 2012;32:425–36.
12. Vermeer SE, Longstreth WT Jr, Koudstaal PJ. Silent brain infarcts: a systematic review. Lancet Neurol. 2007;6:611–9.

13 de Leeuw FE, de Groot JC, Achten E, Oudkerk M, Ramos LM, Heijboer R, Hofman A, Jolles J, van Gijn J, Breteler MM. Prevalence of cerebral white matter lesions in elderly people: a population based magnetic resonance imaging study The Rotterdam Scan Study. J Neurol Neurosurg Psychiatry. 2001;70:9–14.
14. Yue NC, Arnold AM, Longstreth WT Jr, Elster AD, Jungreis CA, O'Leary DH, Poirier VC, Bryan RN. Sulcal, ventricular, and white matter changes at MR imaging in the aging brain: data from the cardiovascular health study. Radiology. 1997;202:33–9.
15. Longstreth WT Jr, Bernick C, Manolio TA, Bryan N, Jungreis CA, Price TR. Lacunar infarcts defined by magnetic resonance imaging of 3660 elderly people: the Cardiovascular Health Study. Arch Neurol. 1998;55:1217–25.
16. Silbert LC, Nelson C, Howieson DB, Moore MM, Kaye JA. Impact of white matter hyperintensity volume progression on rate of cognitive and motor decline. Neurology. 2008;71:108–13.
17. Sachdev P, Wen W, Chen X, Brodaty H. Progression of white matter hyperintensities in elderly individuals over 3 years. Neurology. 2007;68:214–22.
18. Schmidt R, Ropele S, Enzinger C, Petrovic K, Smith S, Schmidt H, Matthews PM, Fazekas F. White matter lesion progression, brain atrophy, and cognitive decline: the Austrian stroke prevention study. Ann Neurol. 2005;58:610–6.
19. Lee S, Viqar F, Zimmerman ME, Narkhede A, Tosto G, Benzinger TL, Marcus DS, Fagan AM, Goate A, Fox NC, Cairns NJ, Holtzman DM, Buckles V, Ghetti B, McDade E, Martins RN, Saykin AJ, Masters CL, Ringman JM, Ryan NS, Frster S, Laske C, Schofield PR, Sperling RA, Salloway S, Correia S, Jack C, Weiner M, Bateman RJ, Morris JC, Mayeux R, Brickman AM. White matter hyperintensities are a core feature of Alzheimer's disease: evidence from the dominantly inherited Alzheimer network. Ann Neurol. 2016;79:929–39.
20. Ramirez J, McNeely AA, Berezuk C, Gao F, Black SE. Dynamic progression of white matter hyperintensities in Alzheimer's disease and normal aging: results from the Sunnybrook Dementia Study. Front Aging Neurosci. 2016;8:62.
21. Yang Z, Wen W, Jiang J, Crawford JD, Reppermund S, Levitan C, Slavin MJ, Kochan NA, Richmond RL, Brodaty H, Trollor JN, Sachdev PS. Age-associated differences on structural brain MRI in nondemented individuals from 71 to 103 years. Neurobiol Aging. 2016;40:86–97.
22. Gouw AA, Seewann A, Vrenken H, van der Flier WM, Rozemuller JM, Barkhof F, Scheltens P, Geurts JJ. Heterogeneity of white matter hyperintensities in Alzheimer's disease: post-mortem quantitative MRI and neuropathology. Brain. 2008;131:3286–98.
23. Park M, Moon Y, Han SH, Kim HK and Moon WJ. Myelin loss in white matter hyperintensities and normal-appearing white matter of cognitively impaired patients: a quantitative synthetic magnetic resonance imaging study. Eur Radiol. 2019;29(9):4914–4921.
24. Bagi Z, Brandner DD, Le P, McNeal DW, Gong X, Dou H, Fulton DJ, Beller A, Ngyuen T, Larson EB, Montine TJ, Keene CD, Back SA. Vasodilator dysfunction and oligodendrocyte dysmaturation in aging white matter. Ann Neurol. 2018;83:142–52.
25. Back S, Kroenke C, Sherman L, Lawrence G, Gong X, Taber E, Sonnen J, Larson E, Montine T. White matter lesions defined by diffusion tensor imaging in older adults. Ann Neurol. 2011;70:465–76.
26. Faraco G, Sugiyama Y, Lane D, Garcia-Bonilla L, Chang H, Santisteban MM, Racchumi G, Murphy M, Van Rooijen N, Anrather J, Iadecola C. Perivascular macrophages mediate the neurovascular and cognitive dysfunction associated with hypertension. J Clin Investig. 2016;126:4674–89.
27. Montine TJ, Phelps CH, Beach TG, Bigio EH, Cairns NJ, Dickson DW, Duyckaerts C, Frosch MP, Masliah E, Mirra SS, Nelson PT, Schneider JA, Thal DR, Trojanowski JQ, Vinters HV, Hyman BT, National Institute on A and Alzheimer's A. National Institute on Aging-Alzheimer's Association guidelines for the neuropathologic assessment of Alzheimer's disease: a practical approach. Acta Neuropathol. 2012;123:1–11.
28. Hyman BT, Phelps CH, Beach TG, Bigio EH, Cairns NJ, Carrillo MC, Dickson DW, Duyckaerts C, Frosch MP, Masliah E, Mirra SS, Nelson PT, Schneider JA, Thal DR, Thies B, Trojanowski JQ, Vinters HV, Montine TJ. National Institute on Aging-Alzheimer's Association guidelines for the neuropathologic assessment of Alzheimer's disease. Alzheimers Dement. 2012;8:1–13.
29. White L, Petrovitch H, Hardman J, Nelson J, Davis DG, Ross GW, Masaki K, Launer L, Markesbery WR. Cerebrovascular pathology and dementia in autopsied Honolulu-Asia Aging Study participants. Ann N Y Acad Sci. 2002;977:9–23.
30. Sonnen JA, Santa Cruz K, Hemmy LS, Woltjer R, Leverenz JB, Montine KS, Jack CR, Kaye J, Lim K, Larson EB, White L, Montine TJ. Ecology of the aging human brain. Arch Neurol. 2011;68:1049–56.
31. Launer LJ, Hughes TM, White LR. Microinfarcts, brain atrophy, and cognitive function: the Honolulu Asia Aging Study Autopsy Study. Ann Neurol. 2011;70:774–80.
32. Beleznai T, Feher A, Spielvogel D, Lansman SL, Bagi Z. Arginase 1 contributes to diminished coronary arteriolar dilation in patients with diabetes. Am J Physiol Heart Circ Physiol. 2011;300:H777–83.
33 Cassuto J, Dou H, Czikora I, Szabo A, Patel VS, Kamath V, Belin de Chantemele E, Feher A, Romero MJ, Bagi Z. Peroxynitrite disrupts endothelial caveolae leading to eNOS uncoupling and diminished flow-mediated dilation in coronary arterioles of diabetic patients. Diabetes. 2014;63:1381–93.
34. McNeal DW, Brandner DD, Gong X, Postupna NO, Montine TJ, Keene CD, Back SA. Unbiased stereological analysis of reactive astrogliosis to estimate age-associated cerebral white matter injury. J Neuropathol Exp Neurol. 2016;75:539–54.
35. Basser PJ, Pierpaoli C. Microstructural and physiological features of tissues elucidated by quantitative-diffusion-tensor MRI. J Magn Reson B. 1996;111:209–19.
36. Yushkevich PA, Piven J, Hazlett HC, Smith RG, Ho S, Gee JC, Gerig G. User-guided 3D active contour segmentation of anatomical structures: significantly improved efficiency and reliability. Neuroimage. 2006;31:1116–28.
37. Zlokovic BV, Gottesman RF, Bernstein KE, Seshadri S, McKee A, Snyder H, Greenberg SM, Yaffe K, Schaffer

CB, Yuan C, Hughes TM, Daemen MJ, Williamson JD, Gonzalez HM, Schneider J, Wellington CL, Katusic ZS, Stoeckel L, Koenig JI, Corriveau RA, Fine L, Galis ZS, Reis J, Wright JD, Chen J. Vascular contributions to cognitive impairment and dementia (VCID): a report from the 2018 National Heart, Lung, and Blood Institute and National Institute of Neurological Disorders and Stroke Workshop. Alzheimers Dement. 2020;16:1714–33.
38. Wu EX, Tang H, Asai T, Yan SD. Regional cerebral blood volume reduction in transgenic mutant APP (V717F, K670N/M671L) mice. Neurosci Lett. 2004;365:223–7.
39. Bennett RE, Robbins AB, Hu M, Cao X, Betensky RA, Clark T, Das S, Hyman BT. Tau induces blood vessel abnormalities and angiogenesis-related gene expression in P301L transgenic mice and human Alzheimer's disease. Proc Natl Acad Sci U S A. 2018;115:E1289–98.
40. Paris D, Humphrey J, Quadros A, Patel N, Crescentini R, Crawford F, Mullan M. Vasoactive effects of A beta in isolated human cerebrovessels and in a transgenic mouse model of Alzheimer's disease: role of inflammation. Neurol Res. 2003;25:642–51.
41. Bevan R, Dodge J, Nichols P, Poseno T, Vijayakumaran E, Wellman T, Bevan JA. Responsiveness of human infant cerebral arteries to sympathetic nerve stimulation and vasoactive agents. Pediatr Res. 1998;44:730–9.
42. Toth P, Rozsa B, Springo Z, Doczi T, Koller A. Isolated human and rat cerebral arteries constrict to increases in flow: role of 20-HETE and TP receptors. J Cereb Blood Flow Metab. 2011;31:2096–105.
43. Longden TA, Dabertrand F, Koide M, Gonzales AL, Tykocki NR, Brayden JE, Hill-Eubanks D, Nelson MT. Capillary K(+)-sensing initiates retrograde hyperpolarization to increase local cerebral blood flow. Nat Neurosci. 2017;20:717–26.
44 Mughal A, Harraz OF, Gonzales AL, Hill-Eubanks D, Nelson MT. PIP2 improves cerebral blood flow in a mouse model of Alzheimer's disease. Function (Oxf). 2021;2:zqab010.
45. Presa JL, Saravia F, Bagi Z, Filosa JA. Vasculo-neuronal coupling and neurovascular coupling at the neurovascular unit: impact of hypertension. Front Physiol. 2020;11: 584135.
46 Pantoni L, Garcia JH, Gutierrez JA. Cerebral white matter is highly vulnerable to ischemia. Stroke. 1996;27:1641–6. discussion 1647
47. Baburamani AA, Ek CJ, Walker DW, Castillo-Melendez M. Vulnerability of the developing brain to hypoxic-ischemic damage: contribution of the cerebral vasculature to injury and repair? Front Physiol. 2012;3:424.
48. Niwa K, Kazama K, Younkin L, Younkin SG, Carlson GA, Iadecola C. Cerebrovascular autoregulation is profoundly impaired in mice overexpressing amyloid precursor protein. Am J Physiol Heart Circ Physiol. 2002;283:H315–23.
49. Faraci FM, Heistad DD. Regulation of the cerebral circulation: role of endothelium and potassium channels. Physiol Rev. 1998;78:53–97.
50. Iadecola C. Untangling neurons with endothelial nitric oxide. Circ Res. 2016;119:1052–4.
51. Iadecola C, Zhang F, Niwa K, Eckman C, Turner SK, Fischer E, Younkin S, Borchelt DR, Hsiao KK, Carlson GA. SOD1 rescues cerebral endothelial dysfunction in mice overexpressing amyloid precursor protein. Nat Neurosci. 1999;2:157–61.
52. Kim HJ, Kim JH, Chae SC, Park YC, Kwon KS, Hong ST. Soluble oligomeric Abeta disrupts the protein kinase C signaling pathway. NeuroReport. 2004;15:503–7.
53. Park L, Anrather J, Forster C, Kazama K, Carlson GA, Iadecola C. Abeta-induced vascular oxidative stress and attenuation of functional hyperemia in mouse somatosensory cortex. J Cereb Blood Flow Metab. 2004;24:334–42.
54. Tong XK, Nicolakakis N, Kocharyan A, Hamel E. Vascular remodeling versus amyloid beta-induced oxidative stress in the cerebrovascular dysfunctions associated with Alzheimer's disease. J Neurosci. 2005;25:11165–74.
55. Han BH, Zhou ML, Abousaleh F, Brendza RP, Dietrich HH, Koenigsknecht-Talboo J, Cirrito JR, Milner E, Holtzman DM, Zipfel GJ. Cerebrovascular dysfunction in amyloid precursor protein transgenic mice: contribution of soluble and insoluble amyloid-beta peptide, partial restoration via gamma-secretase inhibition. J Neurosci. 2008;28:13542–50.
56. d'Uscio LV, He T, Santhanam AV, Katusic ZS. Endothelium-specific amyloid precursor protein deficiency causes endothelial dysfunction in cerebral arteries. J Cereb Blood Flow Metab. 2018;38:1715–26.
57. Santhanam AV, d'Uscio LV, He T, Das P, Younkin SG, Katusic ZS. Uncoupling of endothelial nitric oxide synthase in cerebral vasculature of Tg2576 mice. J Neurochem. 2015;134:1129–38.
58. Park L, Zhou P, Pitstick R, Capone C, Anrather J, Norris EH, Younkin L, Younkin S, Carlson G, McEwen BS, Iadecola C. Nox2-derived radicals contribute to neurovascular and behavioral dysfunction in mice overexpressing the amyloid precursor protein. Proc Natl Acad Sci U S A. 2008;105:1347–52.
59. Miller AA, Drummond GR, Sobey CG. Novel isoforms of NADPH-oxidase in cerebral vascular control. Pharmacol Ther. 2006;111:928–48.
60. Wardlaw JM, Valdes Hernandez MC, Munoz-Maniega S. What are white matter hyperintensities made of? Relevance to vascular cognitive impairment. J Am Heart Assoc. 2015;4: 001140.
61. Prins ND, Scheltens P. White matter hyperintensities, cognitive impairment and dementia: an update. Nat Rev Neurol. 2015;11:157–65.
62. Nokkari A, Abou-El-Hassan H, Mechref Y, Mondello S, Kindy MS, Jaffa AA, Kobeissy F. Implication of the Kallikrein-Kinin system in neurological disorders: quest for potential biomarkers and mechanisms. Prog Neurobiol. 2018;165–167:26–50.
63. Kim KJ, Iddings JA, Stern JE, Blanco VM, Croom D, Kirov SA, Filosa JA. Astrocyte contributions to flow/pressure-evoked parenchymal arteriole vasoconstriction. J Neurosci. 2015;35:8245–57.
64. Kim KJ, Ramiro Diaz J, Iddings JA, Filosa JA. Vasculo-neuronal coupling: retrograde vascular communication to brain neurons. J Neurosci. 2016;36:12624–39.